The International Journal of Engineering and Science (IJES)
|| Volume || 7 || Issue || 5 Ver. II || Pages || PP 01-07 || 2018 ||
ISSN (e): 2319 – 1813 ISSN (p): 23-19 – 1805

Mathematical Techniques In PET

Muhammad Hanif [1], Mohammed Nizam Uddin[2], A.N.M Rezaul Karim[3]
[1]*Professor,* [2]*Assistant Professor*
Department of Applied Mathematics, Noakhali Science and Technology University, Noakhali 3814, Bangladesh
[3]*Associate Professor, Department of Computer Science and Engineering, International Islamic University Chittagong, Kumira, Chittagong, Bangladersh*
Corresponding Author: Muhammad Hanif

----------ABSTRACT----------
Positron emission tomography (PET) is a sophisticated imaging method enabling the provision of relatively precise two-dimensional or three-dimensional data on spatial distribution of a radionuclide inside the object, e.g., a patient's body. It utilizes radioactive decay of a particular type that involves positron emission. This technique is currently in use in astronomy. It's adaptation to PET is non-trivial because of the vastly different source distributions and geometry and basic calculus involved. In this paper we formulate the principles and the mathematical models of PET. Some clinical applications of this modality also discussed in the paper.
KEYWORDS: *Imaging, Basic Mathematics*

Date of Submission: 05-05-2018 Date of acceptance: 21-05-2018

I INTRODUCTION

The development of positron emission tomography (PET) illustrates how advances in basic science translate into benefits for human beings. In 1930 Ernest Lawrence and co-workers conceived of the cyclotron. By 1938 Lawrence, Livingston, et al had designed a "medical cyclotron." The subsequent production of C-11, N-13, O-15, and F-18 found many uses in medical and physiologic research. The introduction of F-18 deoxyglucose represents another major step toward practical clinical use of positron-emitting tracers. In the early 1950's, when workers in Boston first realized the medical imaging possibilities of a particular class of radioactive isotopes. Whereas most radioactive isotopes decay by release of a gamma ray and electrons, some decay by the release of a positron. A positron can be thought of as a positive electron. Widespread interest and acceleration in PET technology was stimulated by development of reconstruction algorithms associated with x-ray CT and improvements in nuclear detector technologies. By the mid-1980s, PET had become a tool for medical diagnosis, for dynamic studies of human metabolism and for studies of brain activation. The positron emission-based imaging utilizes the production of the photon pair to improve substantially the collimation definition of the measured beam.

II PRINCIPLE

Positron emission tomography (PET) is a sophisticated imaging method enabling the provision of relatively precise two-dimensional or three-dimensional data on spatial distribution of a radionuclide inside the object, e.g., a patient's body. It utilizes radioactive decay of a particular type that involves positron emission.

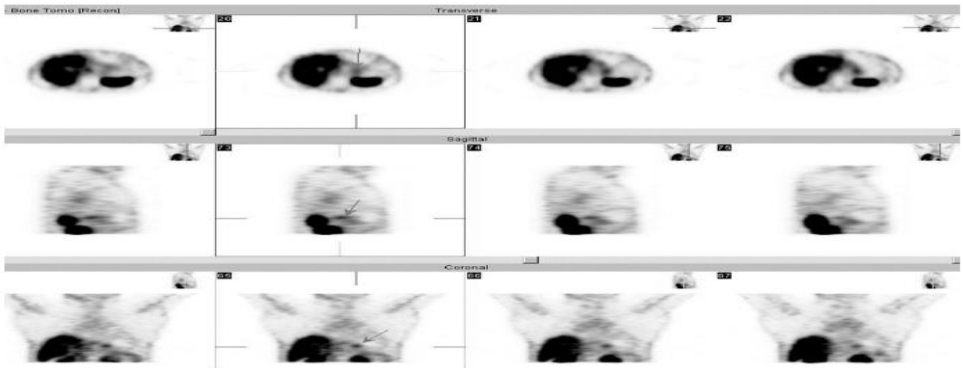

Figure 1 Example of a set of SPECT slices (note the slice orientation indicated on miniature torsi). (Courtesy of the Faculty Hospital Brno-Bohunice, Department of Nuclear Medicine, Assoc. Prof. J. Prasek, M.D., Ph.D.)

An individual phenomenon of such decay consists of several phases important from the imaging aspect (*figure 2*). Initially, a nucleus undergoes a decay producing (besides other decay products) a positron with a certain kinetic energy. Though positrons, as antimatter particles, tend to annihilate in the environment of matter particles, this cannot be accomplished before the positron loses the kinetic energy by colliding with the surrounding medium, thus traveling a certain distance from the place of its origin. The distanceis random and its mean value, dependent on the type of the radionuclide as well as on the surrounding matter, is called *mean positron range* (about 1.4 to 4 mm for different radionuclides in water or soft tissue; less in bones, but much more in lungs). Because the position of the decaying nucleus should be imaged while the location of the

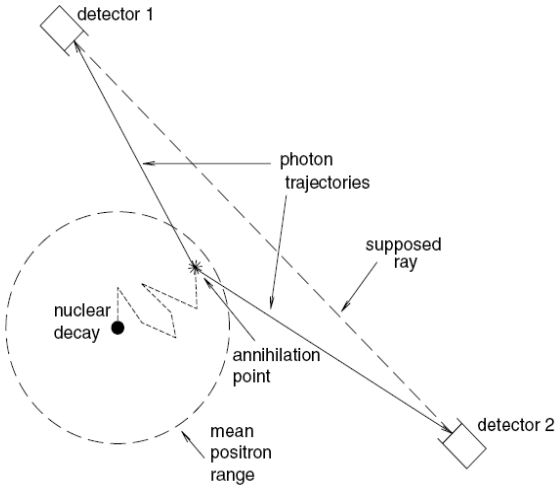

Figure 2 Photon-pair emission in a positron-decay radionuclide and its detection. annihilation is obtained instead, this uncertainty causes a blur in the resulting image denoted as positron range blurring.

The positron finally meets with an electron, which leads to annihilation, producing two high-energy (511-keV) photons traveling in exactly opposite directions. The movement of the positron and electron before annihilation leads to the result that, in the imaging coordinate system, the angle between both photon trajectories need not be exactly 180°, but may differ randomly in the range of about $\pm 0.5°$. This angle is neither measurable nor predictable; thus, the best estimate is the zero mean, i.e., the assumption that the photon trajectories lie on a single line—a ray— crossing the annihilation point. Nevertheless, the related uncertainty contributes to the blur of the image as noncollinearity blurring.

The image data measurement is based, in principle, on coincident detection of both photons by two opposite detectors, as photon travel time of the order of 1 nsec is negligible. Thus, a pair of photons is supposed to be a product of an annihilation event, if the photons are detected at the same time (more precisely, inside a used time window Δt allowing for inexact equality of both detector responses, that is, on the order of 10 nsec). Besides such pairs forming the measured data—true coincident counts—the detectors respond also to individual photons hitting them nonsimultaneously; these events are not considered in the raw count. Nevertheless, they are detected, contributing to a single-count rate for each detector: S_1 and S_2 for detectors D_1 and D_2, respectively. Given the nonzero time window Δt, there will obviously be a certain amount of random coincident counts, which appear when two independent photons are registered simultaneously, though they originated from different annihilations. The random count rate R_c is obviously proportional to the time window and both singlecount rates,

$$R_c = 2\Delta t\, S_1 S_2 \tag{1}$$

The random counts would add an error to every measured value so that a correction is desirable and usually done based on auxiliary measurements.

The detectors used in PET imaging are basically the same as those used in gamma imaging, including SPECT—scintillating crystals with photomultiplier tubes. Naturally, they must be adapted to a higher energy of photons; i.e., crystals with a higher atomic number are used and their dimensions along the expected photon trajectory are greater to ensure high enough photon efficiency. This is very important: a coincident detection requires that both photons interact with the crystal matter and be detected. As both interactions are independent, the probability of the coincident event being detected is given by squared photon efficiency of a single detector that should therefore be close to 1.

Not only does the detection concern unscattered pairs of collinear photons (as is the ideal case), but also the coincident detection may appear for a pair of photons that, though originating from a single annihilation, underwent a Compton scatter (one or both of them, single or multiple scatter). They are then not moving along the original ray, and the line connecting the detectors does not contain the annihilation point, which leads to false image data—*scattered coincident counts*—increasing the measurement noise. The scattered count rate can be substantially reduced by amplitude-discriminating the detector responses, as in gamma cameras, thus rejecting the photons with energy outside of the 511-keV photopeak window.

The measurement should provide a quantity proportional to the total radioactivity on the line between the detectors, i.e., the line integral of the radionuclide spatial density, generalized from equation 1, i.e., along the line D connecting both detectors,

$$P = \int_D \rho(r)\,dr \tag{2}$$

This would be given by the coincident counts if there were no attenuation.

Nevertheless, as in previous sections the emitted γ-photons are attenuated in the sense that there is only a certain probability less than 1 of the photon reaching the respective detector even when traveling originally in the proper direction. This probability is given by the attenuation a on the way d between the annihilation point and the detector input window. For the photon reaching the first detector, D_1, of the respective couple, this is expressed by the line integral of the spatially variant attenuation coefficient μ (x, y, z);

$$a_1 = \exp\left(-\int_{d_1} \mu(r)\,dr\right)$$

The probability a_2 of the second photon of the pair reaching the detector D_2 is given by a similar expression, with the integral over the way d_2. As the attenuation events of photons are independent, the probability of both of them reaching the detectors simultaneously is

$$a_1 a_2 = \exp\left(-\int_{d_1} \mu(r)\,dr - \int_{d_2} \mu(r)\,dr\right) = \exp\left(-\int_D \mu(r)\,dr\right) = a_{ray} \tag{.3}$$

substantially lower than 1. This means that the resulting ray count Pray is decreased, with respect to P, proportionally to Pray, which is obviously the total attenuation on the path (ray) between the detectors,

$$p_{ray} = \exp \int_D \mu(r)\,dr \tag{4}$$

We arrived at an important conclusion: the attenuation, while definitely not negligible, is independent of the position of the annihilation on the ray—all the events on the ray are equally influenced by the total ray attenuation. It is then much easier to compensate for the attenuation in PET imaging than in the case of SPECT. Naturally, the attenuation on each ray must be known or determined prior to or after the image data acquisition.
The count is also influenced by the photon effectiveness of used detectors. As the effectiveness with respect to synchronous pair detection is the squared efficiency of a single detector, this individual parameter must be close to 1—much higher than usual for gamma camera detectors. This requirement is in conflict with the need of small size of the detector crystal, as this defines the ray thickness; also, the higher energy of annihilation photons increases the penetration, thus decreasing the probability of interaction with the crystal. Nevertheless, the parameters of detectors are usually given by the system manufacturer and are only indirectly involved in the data processing.

The most important improvement of PET in comparison with SPECT measurement is the much better collimation: the integrating path—the ray—is fully determined by the position of both coincident detectors, and no collimators similar to those used in gamma detectors or gamma cameras are needed. Also, the cross-section of the ray is given only by the size of input windows of the detectors; it does not increase with depth and is thus a much better approximation of the ideal narrow beam.

Imaging Arrangements

In principle, it would be possible to mount the couple of detectors on a shift-rotate mechanism and to provide, step by step, a sufficient number of parallel projections as sets of gradually shifted ray counts, for different rotation angles. From these one dimensional projections of a two-dimensional slice, the two-dimensional cross-sectional image of the spatial radioactivity distribution could be reconstructed. Practically, it would be a heavy-going practice requiring a long time, as only a very small fraction of emitted photon pairs is detected; as the direction of a photon pair trajectory is random, most of them leave unobserved.

Several different arrangements have been designed, some of them based on a couple of opposite gamma cameras equipped for coincident detection. As all the arrangements provide the data on the same principle, we shall restrict ourselves to the most common dedicated PET system, the basis of which is a ring of fixed detectors, as schematically depicted in *figure 3*.

Let us discuss first the simplest case of a single ring formed of densely situated detectors, without any collimators. A ray can be defined by any couple of the detectors, examples being indicated by connecting lines in the figure; each such ray is described by its (*t, q*) coordinates in the Radon space. It is obvious that a set of (almost)

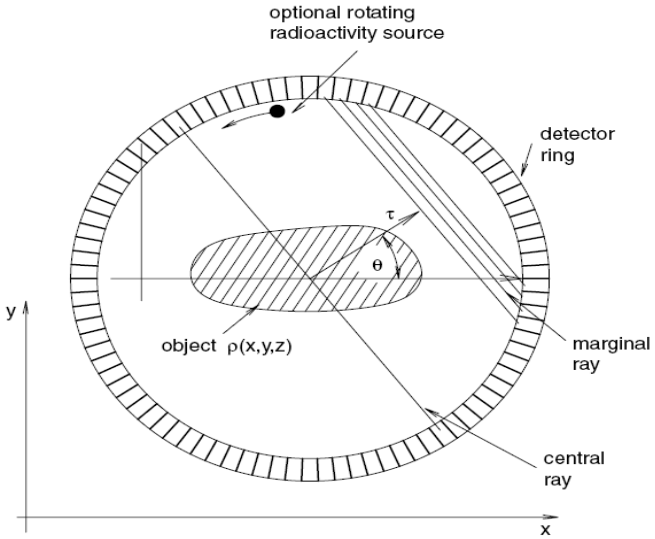

Figure 3 PET detector ring schematically.

parallel lines can be found for each of a number of q angles; the set of counts corresponding to the parallel rays forms a projection. All the detectors in the ring are working simultaneously, but the data are acquired sequentially: a positron decay event in the plane of the circle may generate a photon pair traveling in the plane; such an event is with a high probability detected as a coincidence of two detector responses and should be registered in the system memory. As the directions and positions of the rays belonging to the individual events are random in the measuring sequence, each possible couple of detectors defining a ray has its own bin (location) in the memory that is incremented when the corresponding detection appears.

Obviously, the size of the memory is rather large—a ring with N = 300 detectors defines theoretically N^2 = 90,000 rays (though in practice, the number is somewhat lower, as the rays formed by close detectors are not well defined and should be omitted).

The conflicting requirements on the detector properties result in a compromise, as depicted in *figure 3* in order to achieve a good definition of the rays, the number of detectors on the ring must be high and their width therefore low; on the other hand, to achieve a high photon efficiency, the detector crystal should be thick—thus the radial depth of crystals is rather large. Obviously, the efficiency of the detectors with respect to *g*-photons with oblique trajectory (arriving from the side) is low and the photon may penetrate several neighboring crystals before being detected.

The ring with simultaneously working detectors is obviously much more effective from the viewpoint of photon efficiency than a single detector couple, as all photon pair directions aligned with the slice plane are utilized. Nevertheless, as the photon direction is random, most of the pairs still escape unnoticed. A logical next step in design considerations would be to replace the ring with a spherical (ball) arrangement of detectors, capable of detecting all the ray directions. This is practically unfeasible for obvious reasons, but at least a partial improvement, still enabling good access inside, is possible if more rings are grouped in parallel, thus forming a multilayer detector array (*figure 4*), today mostly limited to about seven to nine layers. Such a detector array can act primarily as a multislice scanner, when each ring is treated separately; however, it can also be considered an approximation of a partial ball arrangement when interslice rays are

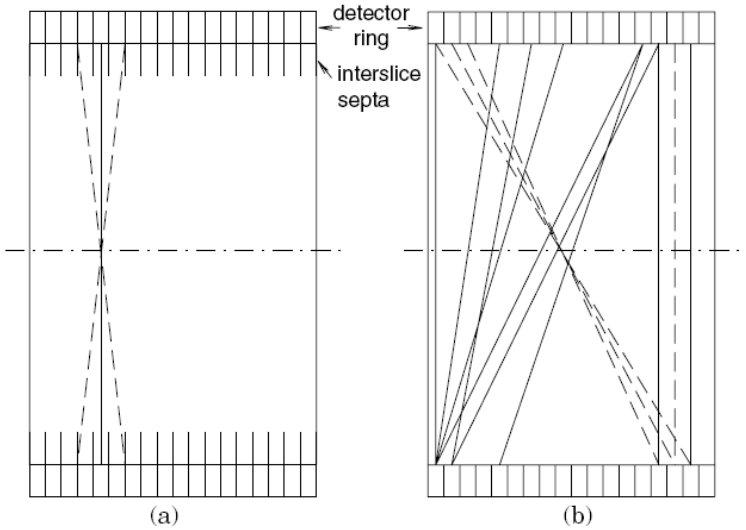

Figure 4 Cross-sectional view of a multislice PET detector array with (a) layer-separating collimators and (b) without collimators.

accepted as well, as indicated by skew lines in *figure 4b*. The total photon effectiveness of the array is higher the greater is covered part of the complete solid angle ($4\pi^2$) which obviously depends on the thickness and number of slices. At the same time, a higher coverage also means more data for true three-dimensional reconstruction, although the measurement is obviously always incomplete and only approximate three-dimensional image reconstruction is possible. On the other hand, this arrangement is naturally more sensitive to scattered photons than an isolated ring, and posterior computational compensation should be applied.

Most multislice PET detector arrays are equipped with removable collimators that, when engaged, separate the individual rings (*figure 4b*). The septa protect the detectors from oblique cross-rays (with a possible tolerance to rays crossing two immediately neighboring rings) and, namely, from scattered photons that might cause higher dead-time ratios and false detections, thus impairing the measurement accuracy. Obviously, only two-dimensional (though multislice) measurement is then possible, but with a better SNR; two dimensional PET imaging is therefore considered to provide better (more reliable) quantitative results.

The PET detector arrays may, in principle, consist of individual detectors arranged on a ring or forming a set of parallel rings. Nevertheless, it would have two drawbacks: (1) a detector with its own photomultiplier is too bulky to allow the placing of a high number of detectors along the ring circumference and may also limit the number of rings on a given axial length of a multislice array, and (2) the cost may be prohibitive. Instead, the equivalently acting principle of block detectors is applied. A single crystal, encompassing the area of several tens of detectors, is deeply cut perpendicularly to its input surface, with the cuts filled by opaque material (*figure 5)*, so that the sections act as individual crystals. However, the light generated by γ -photons

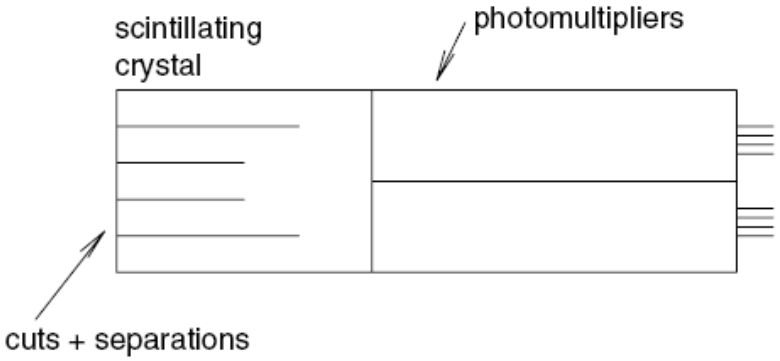

Figure 5 A block detector schematically (outputs on the right).

is distributed in the noncut part of the crystal, as in gamma cameras, and can be measured by only a few (four to six) photomultipliers—the position of interaction (the active subcrystal) being located by basically

Anger logic. From the image data acquisition and processing aspects, this is equivalent to the above-mentioned arrangement of individual detectors.

III MATHEMATICAL MODELS

In PET, radio-isotopes that decay by emitting a positron are used. The annihilation radiation consists of two electromagnetic photons (511 keV photons that are emitted in time coincidence and are oppositely directed). Then one performs coincidence measurements, and hence no collimators are necessary as in SPECT which results in better signal-to-noise ratios.

The drawback of this method is that because of the short half-lives of the isotopes involved a vary expensive cyclotron production facility has to be located near the hospital.

The data measured here are similar to the ones in SPECT but there is one big advantage due to the fact that the photons travel in opposite directions. We get

$$R_{\mu,c}\ f(\omega,s)=\int_{L(\omega,s)} f(x\ )\exp\left[-D\mu(\omega^{\perp},x)+D\mu(-\omega^{\perp},x)\right]dx \tag{5}$$

where L(w, s) is the line $\omega.x$ = s, and because of

$$\left[D\mu(\omega^{\perp},x)+D\mu(-\omega^{\perp},x)\right]=R(\omega,s.\omega) \tag{6}$$

$$R_{\mu,c}\ f(\omega,s)=\ e^{-R\mu(\omega\ ,s)}Rf(\omega,s) \tag{7}$$

and the reconstruction problem is, after dividing by the exponential term, reduced to the one from x-ray computer tomography. Of course the photons emitted are not travelling on a plane so we can immediately use the results from 3D x-ray computer tomography.

IV CLINICAL APPLICATION

Currently, fluordeoxyglucose-F18 (FDG), is the unique PET tracer with clinical applications. FDG is a glucose analogous that penetrates into the cells using sodium-glucose transporters and specific glucose membrane transporters. Once inside the cell, FDG is phosphorylated by the action of hexokinase to FDG-6-phosphate (FDG-6-P) and remains trapped in tissue, whereas glucose is not. From there, FDG-6-P does not follow the metabolic route of glycolysis or glycogen synthesis, being retained in the cell. The physiological or normal distribution of FDG in the organism corresponds to the cellular and tissue consumption of endogenous glucose.

Brain is the organ that shows the major glucose uptake. FDG uptake in heart and skeletal muscles is variable and depends on glucose blood levels (4 - 6 hours fasting, previous to FDG injection, is mandatory), endogenous insulin concentration, and muscular contraction. Bowel uptake is also variable, depending on the peristaltism and muscular tone. There is urinary elimination of FDG; kidneys, ureteral tracts and urinary bladder are visualized in PET images.

Different authors have demonstrated FDG uptake in severely hypoperfused myocardial regions. The flow-metabolism dissociation pattern indicates the presence of ischemic but viable myocardium. At the moment, FDG uptake measured by PET is considered the gold standard to diagnose myocardial viability. The main application of FDG-PET in cardiovascular pathology is to determine the myocardial viability in patients who will be submitted to coronary surgery. If there is no myocardial viability by PET, patients will be treated medically or included in a transplant waiting list (Schwaiger M and Hicks R, 1991).

It is accepted that FDG-PET is the most exact in vivo imaging methodology to evaluate global and regional cerebral metabolism. In the USA, in September, 2004, the HCFA and Medicare established that FDGPET can be used in those patients with moderate cognitive impairment to make the differential diagnosis between Alzheimer dementia and front-temporal dementia. The evaluation of patients with partial epilepsy, refractory to medical treatments, before the surgery is also recognized as an appropriate use of FDG-PET,. FDG-PET detects, during the interictal phase, the epileptogenous focus as a hypometabolic focal area in the cerebral cortex (Newberg A,2002).

The main applications of FDG PET are related to the diagnosis, staging, therapy monitoring, and prognosis of patients with cancer. PET findings have a direct clinical impact on the patient management. FDG-PET can show the pathological increase in glucose consumption that the tumour cells present in vitro. Phosphatase absence in the tumour cells causes an intense metabolic retention of FDG-6- P. A high contrast between the tumour cell uptake and the healthy cell uptake results in a high detection sensitivity by PET. FDG uptake is related to the high cellularity and the cellular proliferation and, therefore, to the degree of malignancy.

The most aggressive tumours require greater glucose consumption to maintain their accelerated growth, whereas those of low degree have less FDG uptake. Scars and already established necrosis and oedema do not show FDG uptake. PET is a good diagnostic tool in oncology because: first, one can do a whole body study in the same exploratory act; second, it has a great sensitivity for detecting malignant neoplastic tissue, demonstrating tumour infiltration in normal sized lymph nodes and in organs that do not yet present anatomical alterations in CT or MRI; third, the findings are less artefacted by the therapy than those of CT and MRI; thus, PET can distinguish residual post-therapy fibrosis and/or postsurgical anatomical distortion from viable tumour tissue; finally, it has a relatively high negative predictive value, since a normal study almost totally discards malignancy – macroscopic tumour disease. FDG-PET can have applications in several clinical situations: to support a diagnosis of a benign lesion or malignancy in processes detected by other techniques, but with complicated or impossible histological confirmation; to establish the extension of an already known tumour prior to treatment – staging; to differentiate neoplastic tissue from fibrotic residual masses after surgery, chemotherapy and/or radiotherapy; to locate a tumour recurrency suspected by clinical analysis and/or an increase in tumour markers; to do a new study of extension after recurrence diagnosis - re-staging; to evaluate the early therapeutic effects; and to look for the primary tumour in a patient with metastatic disease of unknown origin or para-neoplastic syndrome. In addition, PET may guide needle aspiration or biopsy and allows the definition of the volume of irradiation in radiotherapy planning. Few false negatives have been described. Hyperglycaemia can be a cause for them, due to the competition between FGD and the endogenous glucose. In order to avoid them, FDG must be administered to the patient when glycaemia is lower than 140 mg/dL. It is necessary to remember that FDG uptake can be low in some necrotic, mucinous tumours and in low grade tumours. Tumours of small size – and micrometastases - can also occur unnoticed. It is very difficult to speak about diameter or size thresholds for detection, since PET measures the uptake or contrast ratio between lesion and tissue. This ratio is usually very high in the malignant processes.

ACKNOWLEDGEMENT

The Noakhali Science and Technology University for providing a stimulate environment for research.

REFERENCES

[1]. Budliger, T.E 1995. "PET Instrumentation in the Biomedical Engineering Handbook", *CRC Press*, Boca Ratun, Fla, pp. 1140-1150.

[2]. Muhammad Hanif, Md Khabir Ahmed, 2014. "Mathematical Techniques in SPECT", *Bangladesh J. of Radiology and Imaging*, Volume 22, no 1 pp. 8-13

[3]. Muhammad Hanif, Salauddin Al-Azad, 2009. "Mathematical Techniques in DT-MRI", *USTA*, v 15 no 1 pp. 55-66

[4]. Charles L. Epstein, 2011."The Mathematics of Medical Imaging", Department *of Mathematics*, University of Pennsylvania Philadelphia, PA 19104.

Muhammad Hanif." Mathematical Techniques In PET. " The International Journal of Engineering and Science (IJES) 7.5 (2018): 01-07